J Mol Model (2013) 19:3863–3874
DOI 10.1007/s00894-013-1871-3

ORIGINAL PAPER

Homology modeling and structural comparison of leucine rich repeats of toll like receptors 1-10 of ruminants

Anandan Swathi · Gopal Dhinakar Raj · Angamuthu Raja · Krishnaswamy Gopalan Tirumurugaan

Received: 11 December 2012 / Accepted: 30 April 2013 / Published online: 28 June 2013

Abstract Toll-like receptors (TLRs) are transmembrane receptors composed of extra cellular leucine rich repeats (LRRs) that identify specific pathogen associated molecular patterns triggering a innate immune cascade. The LRR regions of TLR 1–10 proteins of goat (*Capra hircus*), sheep (*Ovis aries*), buffalo (*Bubalus bubalis*) and bovine (*Bos taurus*) were modeled using MODELLER 9v7 tool and validated. The similarities and variations of these 10 TLRs extracellular regions of each species were compared using online servers like FATCAT, SSM and SSAP. It was evident that the LRRs of TLRs like 1, 2, 3 and 6 showed structural convergence with <1 % RMSD deviation while TLRs like 5, 7, 8 and 9 had high divergence. Docking analysis showed that TLR 2, 3 and 7 of all the selected four ruminant species were able to bind with their corresponding ligands like Peptidoglycan (PGN), Poly I:C, Resiquimod (R-848) and Imiquimod. However, there were variations in the active site regions, interacting residues and the number of bonded interactions. Variations seen among TLR structures and their ligand binding characteristics is likely to be responsible for species and breed specific genetic resistance observed among species or breeds.

Keywords Docking · Homology model · Leucine rich repeats (LRR) · Rumen species · Toll-like receptors (TLR)

Introduction

Toll-like receptors (TLRs) are evolutionarily conserved innate receptors expressed in various immune and non-immune cells of the mammalian host [1]. As pattern recognition receptors (PRRs), TLRs interact with molecular components of bacterial, viral and fungal organisms that collectively are called pathogen-associated molecular patterns (PAMPs) [2]. These PRRs recognize various PAMPs in various cell compartments and trigger the release of inflammatory cytokines and type I interferons for host defense [1].

Different classes of TLRs, recognize distinct microbial components. TLR2 is the receptor for bacterial lipopeptides, TLR4 detects bacterial lipopolysaccharide, TLR3 double stranded RNA, whereas TLR7/8 and TLR9 recognize single-stranded RNA and unmethylated DNA with CpG motifs respectively [3]. The ligand recognition regions of TLR3, 7, 8 and 9, are located in the endosomal compartment within the cytoplasm whereas the bacterial and fungal ligand recognition regions on TLR1, 2, 4, 5, 6 and 10 are found on the cell surface [4].

TLRs which are type I membrane glycoproteins consist of extracellular leucine rich repeats (LRRs) that are required for PAMP recognition, and a cytoplasmic toll/interleukin-1 receptor (TIR) domain, required for downstream signaling. TLRs have a unique horseshoe, or "m" shaped architecture [5]. All TLR extracellular domain (ECDs) are constructed of tandem copies of LRRs, which is typically 22–29 residues in length and contains hydrophobic residues spaced at distinctive intervals. To date, the structures of ECDs of TLRs 1,

Electronic supplementary material The online version of this article (doi:10.1007/s00894-013-1871-3) contains supplementary material, which is available to authorized users.

A. Swathi · A. Raja
Department of Animal Biotechnology, Madras Veterinary College, Tamil Nadu Veterinary and Animal Sciences University, 600 007, Chennai, India

G. Dhinakar Raj (✉) · K. G. Tirumurugaan
Translational Research Platform for Veterinary Biologicals, Tamil Nadu Veterinary and Animal Sciences University (TANUVAS), Chennai 600 051, India
e-mail: naiptlr@gmail.com

2, 3, 4 and 6 (human or mouse) has been reported [6]. TLR ligands represent all known pathogens and bind by diverse modes to overall structurally similar receptor extracellular domains, leading to the recruitment of adaptors that initiate signaling cascades [7].

There is a lack of extensive structural knowledge regarding the ECDs of important TLRs like 5, 7, 8, and 9 [6]. In the absence of experimental structures, computational methods are used to predict 3D protein models to provide insight into the structure and function of these proteins. To date, homology modeling has been successfully used to identify hits using high-throughput docking (HTD), to suggest accurate binding modes and ligand: receptor interactions, aid in mutagenesis experiments, rationalize SAR data and guide to identify potential ligands [8]. The basis of homology modeling is that two evolutionarily related proteins share a common structure. This approach has been further extended, noting that related proteins bind similar ligands. Frequently, the ligands bound by related proteins are different, but often share a common core substructure [9]. Based on this concept, this study focuses on establishing the LRR structure of TLR 1–10 in few animal species like goat (*Capra hircus*), sheep (*Ovis aries*), buffalo (*Bubalus bubalis*) and bovine (*Bos taurus*) through computational homology modeling and also to find their ligand recognition using HTD.

The ECD of human TLRs 7, 8 and 9 has been modeled, based on the crystal structure of TLR 3, to identify functionally important residues [3] and their LRR regions, using the template segment assembly approach [10]. Other TLRs like TLR 8 from rodent and non rodents were modeled using comparative homology modeling and its docking interactions were studied with R-848 compound to understand the species specific signaling pathway. A protein model for hTLR 10 structure was developed using hTLR1 as template and its binding activity with ligands like Pam3CSK4 and PamCysPamSK4 were analyzed [11]. Ectodomain models of human TLR5, TLR6, TLR7, TLR8, TLR9, TLR10 and mouse TLR1, TLR11, and TLR12 were done through Leucine-rich repeat assembly approach [12]. While most of the modeling and docking studies were based on human and mouse TLRs, this is the first report to be on rumen TLRs.

Methodology

Retrieval of sequences

TLR 1–10 full length protein sequences of goat (*Capra hircus*), sheep (*Ovis aries*), buffalo (*Bubalus bubalis*) and bovine (*Bos taurus*) were retrieved from NCBI protein database (http://www.ncbi.nlm.nih.gov/). SMART tool (http://smart.embl-heidelberg.de) was used to find the domain architecture, signal peptides and LRR repeats in the query sequence. Since the objective is to model the LRR structure of TLRs, the LRR sequences were alone separated from the whole protein sequence. This sequence was then subjected to Blastp (version 2.2.17) to obtain the template for modeling the 3D structure of TLRs LRR. The search was performed against Protein Data Bank (PDB) using default parameters. Based on high sequence similarity and lower E-value, the best templates were selected for each TLR. The accession numbers for individual TLR's and their corresponding suitable templates are mentioned in the Supplementary File 1. The template structures were obtained from the PDB database (http://www.rcsb.org).

Generation of 3D structures through homology modeling

MODELLER 9v7 was used to perform the homology modeling. MODELLER tool implements comparative protein structure modeling by satisfaction of spatial restraints. The spatial constraints include distances, angles, dihedral angles, pairs of dihedral angles and other spatial features defined by atoms and pseudo atoms [13]. ClustalW [14] was used to align the target and template sequences and the resultant alignment was stored as PIR format. The alignment file, template file (pdb format) and the supported python script files were given as input to the MODELLER 9v7 software. For each TLR of a single animal species, five templates were selected to obtain the best modeled 3D LRR structure. Hence the modeler tool was run 200 times (40 proteins × 5 templates) to obtain good models for the 40 TLR structures, i.e., 10 TLR proteins in four animal species. 3D optimized models are generated at the end of modeling through molecular probability density function (molpdf).

Evaluation of homology modeled proteins

The generated models were evaluated using five different tools like Procheck, ERRAT, Verify 3D (http://nihserver.mbi.ucla.edu/SAVES/), WHATIF server (http://swift.cmbi.ru.nl/servers/html/index.html) and ProQ (http://www.sbc.su.se/~bjornw/ProQ/ProQ.html). The stereochemical quality and the overall structural geometry of the generated models were evaluated by the Ramachandran plot of Procheck [15]. Other factors like the statistical parameters of non bonded interactions and the structural error values are checked by the ERRAT tool [16]. The compatibility of the 3D homology models with its amino acid sequence are scored by the Verify 3D tool [17]. Furthermore, the Z-score of What if server is used to calibrate the quality check of Ramachandran plots [18]. ProQ is used to predict the accurate models based on the LGscore [19]. The homology modeled TLR LRR proteins were considered as 'good models' only if it satisfied the threshold criteria of at-least three different tools. Discovery Studio software v2.5 was used for optimizing and simulating the validated protein

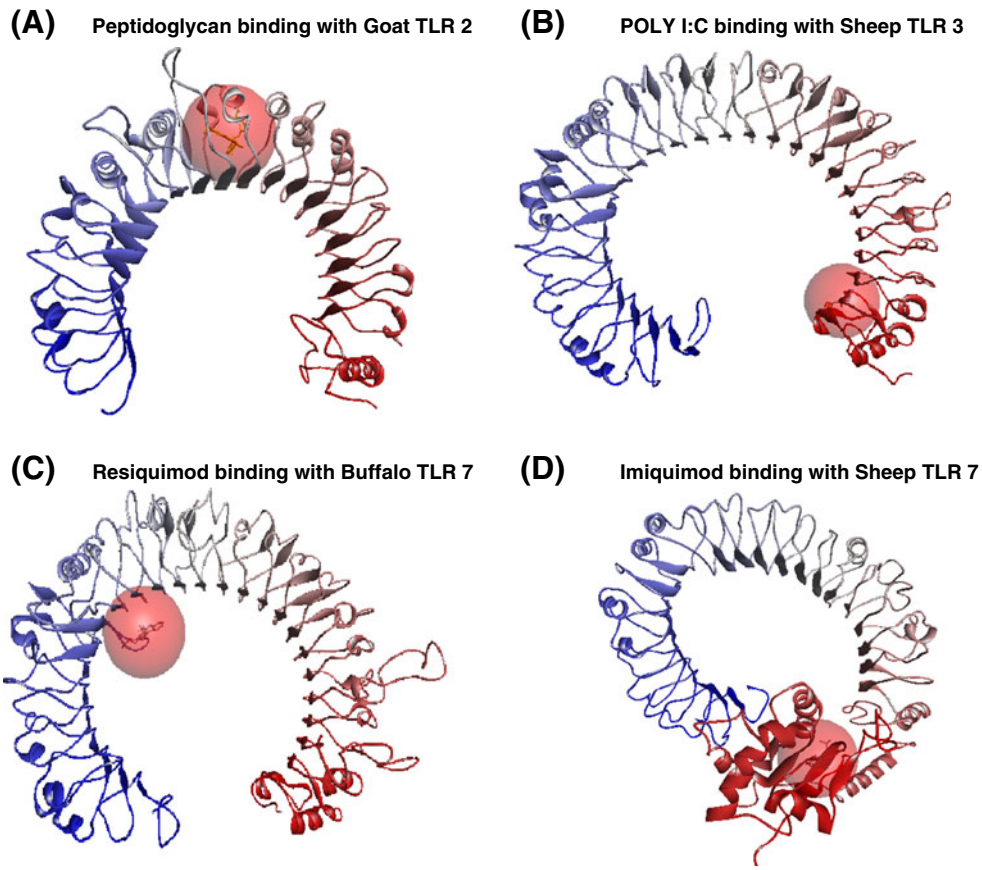

Fig. 1 Docking view

models. The best validated TLR structures were submitted to the Protein Model Database (http://mi.caspur.it/PMDB/) [20].

Comparison of TLR LRR modeled proteins

Comparative modeling is capable of producing accurate structural models for many protein sequences [21]. The modeled LRR structures are compared against the four different animal species by implementing tools like FATCAT (http://fatcat.burnham.org/), SSM server (http://www.ebi.ac.uk/msd-srv/ssm/) and SSAP (http://protein.hbu.cn/cath/cathwww.biochem.ucl.ac.uk/cgi-bin/cath/GetSsapRasmol.html). The structures are compared based on RMSD deviation and other statistical probability scores. Further, the structural superimpositions of the modeled proteins are done using DS Visualizer and the differences in the species level are identified (Figs. 1, 2).

Docking analysis

In order to perform docking, standard analog ligand structures like Peptidoglycan (SID: 4145), Poly I:C (CID: 32744), Resiquimod (R-848) (CID: 159603), Imiquimod (CID: 57469) (Fig. 3) were obtained from Pubchem compound database (http://www.ncbi.nlm.nih.gov/pccompound) and KEGG ligand database (http://www.genome.jp/kegg/ligand.html). The modeled LRR TLR protein structures were considered as receptors. Docking was carried out using Autodock Vina 1.1.5 software. Graphical User Interface program "AutoDock Tools" was used to prepare, run, and analyze the docking simulations. Polar hydrogens were added into the receptor protein and also Gasteiger-Marsili charges were incorporated prior to the docking process. The ligands are modified and saved as PDBQT file. The active binding site was unknown so in order to cover the entire protein and facilitate flexible ligand binding the grid box of x, y, and z-axes were set as 126×126×126 Å. Lamarckian genetic algorithm was chosen to find the ideal conformers. The docked protein complex was analyzed using Molegro molecular viewer (http://www.clcbio.com/products/molegro/) and DS Visualizer (http://accelrys.com/).

Results

TLR LRR sequence retrieval

Toll like receptor 1–10 complete protein sequence from four species goat, sheep, buffalo and bovine was retrieved from the NCBI protein database. The length of the TLR sequences varied from 400–803 amino acids, the highest being TLR 7.

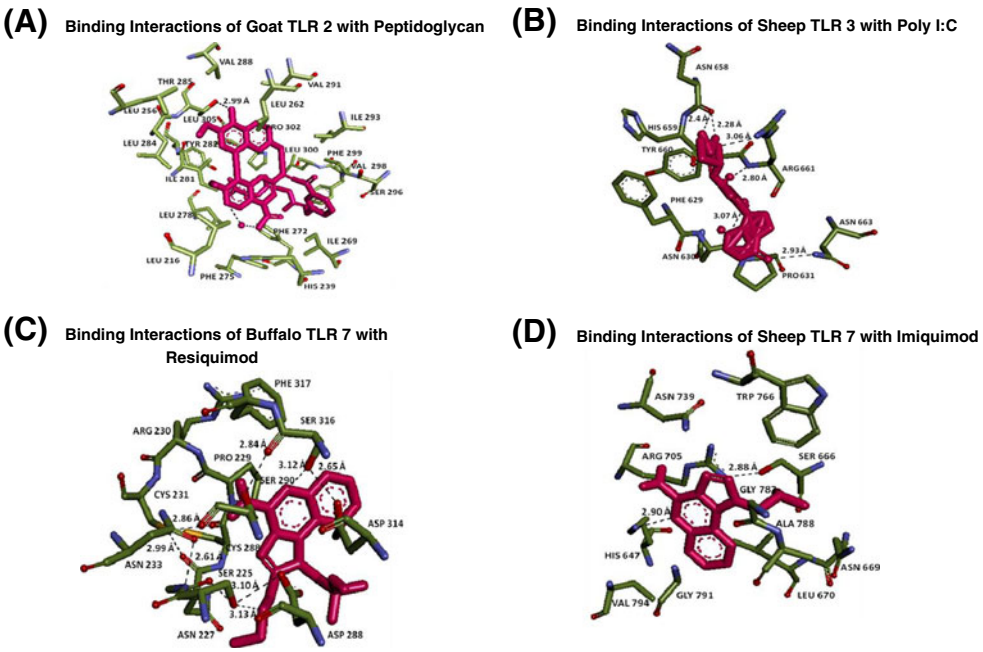

Fig. 2 Best docked structures of Tlr 2, 3 And 7 with their respective ligands

The TIR domain, transmembrane (TM), N-terminal LRR, C-terminal LRR regions were identified using SMART tool. Since the objective is to model the LRR protein structure, the sequences specific to LRR were used from the whole sequence using SMART tool. Blast similarity search was performed to obtain suitable templates. The templates having maximum identity and sequence coverage with lesser E-value were considered for further analysis. The templates were downloaded from the PDB database.

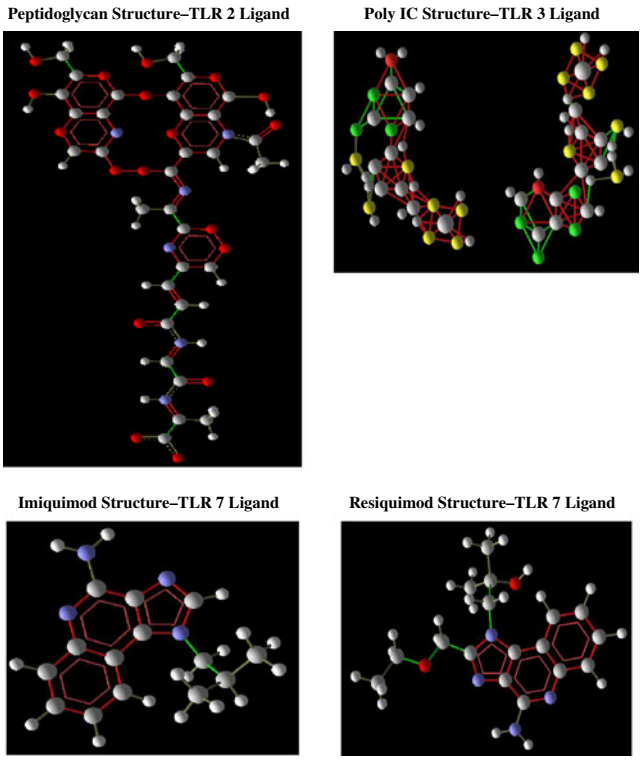

Fig. 3 TLR ligand structures

Homology modeling using MODELLER 9v7:

To obtain the best model for each TLR sequence, five templates were selected which had high level of sequence identity. Homology modeling was performed for all 10 TLRs in four animal species using MODELLER 9v7 tool. The refined homology modeled proteins were selected depending on lowest molpdf energy values. These models were subjected to validation using Procheck, ERRAT, Verify 3D, WHATIF server and ProQ tools. Most of the generated models satisfied the Ramachandran plot stereo-chemical constraints. However on subsequent checking with other tools out of 40 TLR LRR proteins, only 32 protein structures were validated as 'good models' and the remaining eight were rejected based on the threshold criteria. The template selection and the protein model validation values are mentioned in the Supplementary File 1. The validated stereo-chemically fit models were submitted to protein model database. Goat, sheep, buffalo and bovine TLR 1–10 modeled proteins can be accessed via the PMDB ID (Supplementary File 1).

Comparison of LRR structures in TLRs

The comparison of TLR LRR proteins was done using tools like SSM [22], SSAP [23] and FATCAT [24]. All ten TLR LRR structures were compared across species, for example, TLR 1 modeled protein of buffalo was compared with TLR

1 modeled protein of goat, sheep and bovine. This species level comparison was repeated with the other nine TLRs. Table 1 illustrates the relative comparison values of TLR 1–10 modeled proteins in the four animal species.

Docking analysis

Docking analysis was carried out in TLR2, TLR 3 and TLR 7 modeled proteins of goat, sheep, buffalo and bovine. Autodock Vina 1.1.5 software was used to perform the flexible binding analysis. Except with sheep TLR2, peptidoglycan ligand bound with other three TLR 2 proteins. However, only a single hydrogen bond interaction was observed on docking PGN with goat, buffalo and bovine TLR 2 structures. The number of binding sites in the TLR 3 modeled protein varied from 14–19, while in TLR 7 binding sites ranged from 16–29. Poly I:C ligand bound with the modeled protein of goat, sheep, buffalo and bovine with different binding energy values ranging from −7.3 to −8.0 kcal mol^{-1}. Sheep TLR 3-Poly I:C bound complex had the maximum no of hydrogen bonds, i.e., ten while the goat and buffalo Poly I:C complex had a minimal of eight hydrogen interactions. Bovine TLR 3 modeled protein had nine interactions with the ligand (Table 2).

Resiquimod (R-848) is known as a standard ligand compound for TLR 7 protein. Hence docking was carried out with the modeled TLR 7 animal protein against R-848. TLR 7 protein had varied number of binding sites with respect to individual animal species. All the TLR 7 proteins were able to bind with R-848 ligand with lower binding energy values. Goat and sheep TLR 7 had the same binding energy values as −7.1 kcal mol^{-1}, whereas buffalo and bovine had −7.3 and −6.8 kcal mol^{-1} respectively. The number of hydrogen bond interactions with buffalo TLR 7 R-848 complex was 6, goat TLR 7 R-848 complex was 4, sheep and bovine TLR 7 R-848 complex had 3 bonded associations. In TLR 7 of goat, sheep, bovine about 12 interacting amino acids participated toward the binding of R-848 ligand. The binding pattern of TLR 7 was also observed with Imiquimod. The binding energy values of sheep TLR 7 with Imiquimod was −8.1 kcal mol^{-1}; goat and bovine TLR 7 had −7.8 kcal mol^{-1}; buffalo TLR 7 Imiquimod ligand complex displayed with −7.3 kcal mol^{-1} binding energy respectively. On comparison with Resiquimod, Imiquimod showed only 2–3 hydrogen bond associations with TLR 7 complex. Since TLR 8 signaling was found to be activated with synthetic ligand like resiquimod [11], insilico analysis was also performed to confirm the binding with rumen TLR 8 proteins. R-848 compound bound against all the TLR 8 proteins of goat, sheep, buffalo and bovine. However, the docking was observed in different binding sites. This may account for variations between TLR structures (Table 2).

Discussion

There is minimal knowledge about the LRR structural information on animal TLRs. To date, only the structures of ECDs of TLRs 1, 2, 3, 4 and 6 (human or mouse) has been reported [6] and no structure has yet been reported for any member of the TLR 7, 8, and 9 subfamily. Among mammals, members of the TLR gene family carry out a fundamental role in the recognition of PAMPs from bacteria, viruses, protozoa, and fungi, thereafter provoking the modulation of an innate immune response. The LRR-containing ectodomains of the TLR proteins have been hypothesized to facilitate detection of invading PAMPs [25]. To understand this aspect of PAMP recognition in animal TLRs, LRR regions in TLR proteins were modeled in a few animal species like goat, sheep, buffalo and bovine and their recognition with bacterial/viral constituents was observed by computational docking with already established ligand structures.

The LRR motifs are found in many proteins in animals, plants and microorganisms, including many proteins involved in immune recognition [6]. SMART tool was used to detect the presence of these LRRs specific to animal TLR sequences. The result from SMART tool led to the understanding that the TLRs like 3, 7, 8, 9 had consistently high number of LRRs ranging from 13–21, while TLRs like 1, 5, 10 had relatively fewer numbers of LRRs ranging from 6–13. Except goat species, TLR 7 and TLR 9 from sheep, buffalo and bovine did not have a transmembrane domain region. Low-complexity regions are completely absent in TLR7, 8 and TLR9. On analyzing TLRs from 1 to 10 in four animal species, it was found that sheep had the highest number of LRRs followed by buffalo, bovine and goat.

It has been widely reported that LRR family proteins have ligand binding sites on the concave side of their protein structure [26, 27]. In deletion mutagenesis experiments, the N-terminal LRR modules which was deleted contained neither the ligand-binding nor the dimerization region of TLR2 [28]. It has also been observed that TLR2 pocket is formed at the domain boundary between the central and C-terminal regions. The binding of triacylated lipopeptide to TLR2 occurs in a lipid-binding pocket that is formed at the convex face of the junction between the central and C-terminal LRR domains [29]. The docking on rumen TLR 2 with peptidoglycan also showed binding between the central and C-terminal domains.

With respect to TLR3, The dsRNA interacts with both N-terminal and C-terminal sites on the lateral side of the convex surface of TLR3 [30]. Further mutagenesis studies on TLR 3 ECD also revealed a single binding site near the non-glycosylated surface of C terminal region with important residues like H539 and other asparagines which are found to be essential for TLR3 activation [31, 32]. Despite

Table 1 Relative comparison of TLR LRR 1–10 modeled proteins

TLR type	SSM tool				SSAP tool				FATCAT tool			Superimposed (S) OR not superimposed (N)
	Q score	P score	Z score	RMSD	Overlap (%)	Sequence identity (%)	Score	RMSD	P value	RMSD	No of twists	
TLR 1												
Buffalo, goat	0.85	73.7	26	0.96	99	95	95.09	1.69	0	1.86	0	S - similar
Buffalo, sheep	0.88	85.7	27.9	0.65	100	95	95.51	1.82	0	1.82	0	S - similar
Buffalo, bovine	0.88	83.3	27.5	0.84	100	97	95.53	1.69	0	1.3	0	S - similar
TLR 2												
Buffalo, goat	0.94	91.6	28.9	0.51	99	90	95.81	1.18	0	0.85	0	S - similar
Buffalo, sheep	0.91	87.5	28.2	0.64	99	91	95.89	1.29	0	1.1	0	S - similar
Buffalo, bovine	0.93	98	29.9	0.32	94	96	95.37	0.44	0	0.67	0	S - similar
TLR 3												
Buffalo, goat	0.92	92.6	29.2	0.68	98	89	95.41	0.7	0	0.76	0	S - similar
Buffalo, sheep	0.96	114.3	32.3	0.43	100	99	97.03	0.8	0	0.82	0	S - similar
Buffalo, bovine	0.91	94	29.3	0.82	98	95	95.95	1.03	0	0.81	0	S - similar
TLR 4												
Buffalo, goat	0.23	15.5	14.4	1.9	63	58	76.75	7.54	~0	3.02	0	N -dissimilar
Buffalo, sheep	0.92	83.8	27.6	0.87	100	92	96.25	0.89	0	0.89	0	S - similar
Buffalo, bovine	0.97	88.2	28.3	0.27	100	96	97.45	0.41	0	0.41	0	S - similar
TLR 5												
Buffalo, goat	0.31	5.2	10.9	2.42	80	15	80.42	3.17	0	3.06	0	N -dissimilar
Buffalo, sheep	0.18	0	4	3.45	85	36	68.94	12.42	~0	2.79	2	N -dissimilar
Buffalo, bovine	0.14	4.6	10.1	2.85	63	8	68.52	5.32	~0	3.14	3	N -dissimilar
TLR 6												
Buffalo, goat	0.88	73.8	26	0.7	96	83	94.62	0.74	0	0.69	0	S - similar
Buffalo, sheep	0.88	72.6	25.7	0.89	99	96	94.78	1.12	0	1.12	0	S - similar
Buffalo, bovine	0.89	76.2	26.4	0.73	98	91	95.07	1.14	0	1.13	0	S - similar
TLR 7												
Buffalo, goat	0.083	4.2	11.4	2.58	51	6	60.98	9.6	~0	4.06	5	N -dissimilar
Buffalo, sheep	0.13	0	5.2	3.72	64	7	63.03	8.7	~0	3.09	1	N -dissimilar
Buffalo, bovine	0.6	60.9	24.5	1.17	97	84	85.85	5.83	~0	2.84	0	N -dissimilar
TLR 8												
Buffalo, goat	0.06	0	6.3	2.48	51	7	59.86	13.93	~0	3.23	3	N-dissimilar
Buffalo, sheep	0.12	0	4.1	3.36	72	8	65.51	10.19	~0	2.94	2	N-dissimilar
Buffalo, bovine	0.1	0	2	4.43	62	8	59.31	10.12	~0	3.09	3	N-dissimilar
TLR 9												
Buffalo, goat	0.12	0	3.1	3.56	68	6	67.48	7.09	~0	3.13	2	N -dissimilar

Table 1 (continued)

TLR type	SSM tool				SSAP tool			FATCAT tool			Superimposed (S) OR not superimposed (N)
	Q score	P score	Z score	RMSD	Overlap (%)	Sequence identity (%)	Score	RMSD	P value	RMSD	No of twists	
Buffalo, sheep	0.074	0	3.3	4.38	68	6	67.84	6.87	~0	3.1	1	N -dissimilar
Buffalo, bovine	0.069	0	2.2	4.77	55	10	58.66	11	~0	3.07	5	N -dissimilar
TLR 10												
Buffalo, goat	0.78	75.3	26.2	0.72	87	89	92.91	1.1	0	1.03	0	S - similar
Buffalo, sheep	0.19	1	8.3	3.74	84	48	73.7	5.24	~0	3.09	1	N -dissimilar
Buffalo, bovine	0.91	86.1	28	0.72	99	95	94.91	0.85	0	1.19	0	S - similar

the binding site near the C terminal region, there is another dsRNA binding site near the N terminal side with histidine residues [31]. In our study, goat, sheep and buffalo TLR 3 showed poly I:C binding in the central ECD while bovine TLR 3 alone showed ligand binding near the C-terminal region.

Biochemical studies on TLR 7 and TLR 8 reveals that the N-terminal portion of TLR7 is necessary for function but not ligand binding. Also, ligand binding and signal transduction are likely to be separate events for both TLR9 and TLR7 [33]. Docking studies with TLR 7 of goat, buffalo and bovine showed R-848 binding near the N-terminal region, while in sheep TLR 7 showed binding toward the other C-terminal domain. In case of TLR8-R848 complex, goat, sheep and bovine showed binding region in the central ECD region, while buffalo TLR 8 showed binding pocket in the C-terminal side. The docking results analyzed on TLR7 and TLR 8 with resiquimod showed varied binding site regions. TLR 7 of rumen showed different active sites with imiquimod ligand.

Among many techniques, homology modeling is the most successful method for predicting three-dimensional protein structure [9]. Given an experimentally established protein structure (template), models can be generated for a homologous sequence (target) that shares with either the template significant sequence or structural similarity [8]. This approach of homology modeling was applied to model the LRR structures of animal TLRs 1–10 using MODELLER 9v7 tool. On template selection using Blastp, it was found that most of the templates which satisfied the similarity criteria were from *Homo sapiens* (PDB Id: 2Z7X, 2A0Z, 2Z66, 1ZIW, 2Z63, 3J0A, 3ULU)*, Mus musculus* (PDB Id: 2Z81, 3A79, 2Z64) and *Eptatretus burger* (PDB Id: 2Z7X, 2Z81, 2Z66, 3A79, 2Z63, 3 V44). Exceptionally few TLRs like TLR 8 and TLR 9 in goat showed similarity with *Bos taurus* template structure (PDB Id: 1XKU) and bovine TLR 5 had similarity with a protein structure from Zebra fish (PDB Id: 3 V44). The template structures like 2Z7X (human), 2Z81 (mouse), 2A0Z (human), 3A79 (mouse) were constantly repeated to model the TLR LRRs of 1, 2, 3, 6 structures respectively. This denotes that there might be a high level of structural similarity in the TLRs LRR of 1, 2, 3, 6 in the four animal species.

Based on stereo chemical quality, structural similarity and fold quality, MODELLER was found to render better results than other homology modeling tools like MOE, InsightII-Homology and Swiss-PdbViewer (SPV) for modeling membrane proteins [34]. A similar study conducted by a different group concluded that modeler performed marginally better than five different homology tools for overall protein modeling [35]. Due to high efficiency, MODELLER 9v7 was used to model the animal

Table 2 Binding analysis of TLR2, TLR 3, TLR 7 and TLR 8

S. No	Species	TLR Type	Ligand	Total no of binding sites	Total no of interacting residues	Interacting residues	No of hydrogen bonds	Binding energy(kcal mol^{-1})
1	goat	TLR 2	Peptidoglycan	14	20	Leu 216, Phe 275, His 239, Phe 272, Ile 269, Ser 296, Val 298, Phe 299, Leu 300, Val 291, Pro 302, Leu 262, Leu 305, Thr 285, Tyr 282, Leu 284, Ile 281, Leu 278, Leu 256, Val 288	1	−9.8
2	sheep	TLR 2	Peptidoglycan	16	Nil	Nil	Nil	Nil
3	buffalo	TLR 2	Peptidoglycan	12	14	Ile 269, His 239, Ile 264, Phe 234, Phe 216, Ile 281, Leu 278, Pro 302, Val 301, Leu 300, Phe 272, Val 298, Phe 299, Leu 305	1	−8.4
4	bovine	TLR 2	Peptidoglycan	15	17	Val 274, Phe 248, Phe 275, Leu 276, Pro 278, Leu 281, Leu 254, Tyr 258, Ile 257, Thr 261, Leu 260, Ile 240, Ile 269, Leu 243, Ser 272, Ile 245, Leu 238	1	−9.7
3	goat	TLR 3	Poly I:C	15	10	His 269, His 249,Asp 242,Val 243,Phe 244,Val 271,Tyr 252, Val 251,Met 270,Ala 268	8	−7.9
4	sheep	TLR 3	Poly I:C	18	9	Pro 631, Asn 663, Arg 661, Asn 658, His 659, Phe 629, Tyr 660, Asn 630, Phe 632	10	−8.0
5	buffalo	TLR 3	Poly I:C	19	8	Phe 375, Ser 376, Gln 321, Asp 351, Asn 350, Trp 316, Asp 349, Asn 373	8	−7.7
6	bovine	TLR 3	Poly I:C	14	10	Asn 498, Ala 497, Asn 495, Ile 496, Asn 494, Ala 469, Leu 470, Lys 471, Val 473, Asp 474	9	−7.3
7	goat	TLR 7	Resiquimod R-848	29	12	Cys 231, Tyr 232, Asn 202, Phe 236, Gln 248, Ile 204, Asn 203, Ser 245, Lys 175, Asn 244, Asn 173, Gln 145	4	−7.1
8	sheep	TLR 7	Resiquimod R-848	16	12	Ile 602, Leu 603, Arg 605, Trp 604, Asp 606, Lys 613, Asp 608, Lys 568, Arg 610, Phe 614, Glu 594, Asn 598	3	−7.1
9	buffalo	TLR 7	Resiquimod R-848	19	16	Arg 344, Lys 346, Asp 314, Asp 288, Tyr 199, Ser 316, Phe 317, Pro 229, Gln 291, Cys 228, Gly 226, Asn 233, Ser 225, Ser 290, Arg 230, Asn 227	6	−7.3
10	bovine	TLR 7	Resiquimod R-848	18	12	Ile 144, Leu 120, Leu 94, Tyr 96, Ser 122, Glu 124, Tyr 146, Arg 172, Asn 227, Asn 170, Tyr 201, Tyr 199	3	−6.8
11	goat	TLR 7	Imiquimod	29	13	Ile 62, Asp 63, Lys 87, Arg 65, Thr 20, Lys 22, Leu 56, His 54, Asp 18, Phe 53, Ser 52, Ala 51, His 14	2	−7.8
12	sheep	TLR 7	Imiquimod	16	12	Trp 766, Gly 787, Ala 788, Asn 669, Leu 670, Gly 791, Ser 666, Val 794, Lys 647, Arg 705, Pro 737, Asn 739	2	−8.1
13	BUFFALO	TLR 7	Imiquimod	19	11	Gln 149, Asn 150, Leu 174, Lys 175, Ile 204, Pro 235, Thr 239, Pro 237, Tyr 232, Asn 202, Asn 173	2	−7.3
14	bovine	TLR 7	Imiquimod	18	11	Glu 771, Thr 770, Trp 766, Val 764, Trp 762, Val 761, Val 740, Leu 749, Asn 757, Ile 731, Cys 758	3	−7.8
15	goat	TLR 8	Resiquimod	14	16	Ala 318, Leu 309, Pro 349, His 345, Leu 350, Lys 329, Leu 364, Asn 367, Thr 353, Ile 327, Phe 380, Phe 377, Ala 361, Asn 360, Gly 359, Leu 386	1	−8.3

Table 2 (continued)

S. No	Species	TLR Type	Ligand	Total no of binding sites	Total no of interacting residues	Interacting residues	No of hydrogen bonds	Binding energy(kcal mol^{-1})
			R-848					
16	sheep	TLR 8	Resiquimod	14	9	Arg 317, Leu 316, Ser 346, Phe 345, Glu 315, Gln 314, Asn 377, His 374, Gln 373	2	−6.2
			R-848					
17	buffalo	TLR 8	Resiquimod	8	14	Glu 536, Ser 541, Thr 537, Leu 512, Ile 515, Val 508, Ile 505, Phe 485, Asp 482, Phe 503, Arg 504, Asp 530, Leu 534, Thr 533	5	−7.7
			R-848					
18	bovine	TLR 8	Resiquimod	17	11	Leu 396, Thr 399, Thr 446, Asp 384, Leu 434, Gly 427, Ser 435, Asn 433, Leu 432, Asn 428, Ile 429	3	−7.1
			R-848					

TLR LRR structures. Each animal TLR was modeled with a minimum of five different templates. The alignment between the 3D coordinates of the template structure and the target sequence was saved in PIR format using Clustalw. This alignment was then submitted as input to the modeler 9v7 tool. Python scripts were used to generate at-least three protein models. For comparative modeling MODELLER automatically derives restraints from the given related structures and their alignment with the target sequence [36]. MODELLER builds loops by optimizing a series of 'probability density functions' describing backbone geometry based on amino-acid type, and then refined with an energetic minimization procedure [35]. The three dimensional (3D) model is obtained by optimally satisfying spatial restraints derived from the alignment and expressed as probability density functions (pdfs) for the features restrained [13]. From the 3 modeled proteins, the model with the least probability density function value was selected for further analysis (Fig. 1, Supplementary File 2). For optimizing the modeled TLR LRR proteins molecular dynamic simulations were carried out using CHARMm forcefied from Discovery Studio software.

The structurally refined model are validated using different tools like PROCHECK, WHATIF server, ProQ, Verify 3D and ERRAT. The percentage of residues in most favored regions and additional allowed regions were considered by the Ramachandran plot of Procheck. If the overall percentage falls above 95 % then the protein model is considered as a good structure. In the WHATIF server, output for a protein is a Ramachandran Z-score, expressing the quality of the Ramachandran plot relative to current state-of-the-art structures [37]. An experimental study conducted on assessing the quality of proteins on 144142 PDB structures with mean Z score value showed values as −0.58 for X-ray diffraction, −1.19 for NMR and −2.0 for EM[38]. So Z-value of −2 or lower is kept as the threshold for this study. According to this criterion, only 16 out of 40 models satisfied these structural constraints. ProQ, a neural network based method was used to predict the quality of a protein model that extracts structural features, such as frequency of atom–atom contacts, and predicts the quality of a model, as measured either by LGscore or MaxSub. Correct models should have LGscore>1.5 and MaxSub>0.1, whereas incorrect models should have LGscore<1.5 and MaxSub<0.1 [18]. In this study, except for sheep TLR 7 and buffalo TLR 8 all other TLR LRR protein models satisfied the ProQ LGscore threshold. Another protein validation tool named Verify 3D compares the protein model to its own amino-acid sequence, using a 3D profile [39]. On submission of the protein model, this tool automatically computes whether the protein model is passed or failed depending upon the percentage of residues with >0.2 3D-1D score. ERRAT tool works on the statistics of non-bonded interactions between different atom types and calibrates the error function

of the protein model. The reliability of the modeled protein was checked by this tool. Based on the results of these different tools, 36 models were found to be stereo-chemically efficient models while the remaining models like sheep TLR 5, sheep TLR 7, sheep TLR 8 and buffalo TLR 8 did not satisfy the constraints imposed by the validation tools. The validated TLR LRR animal protein models were submitted to PMDB database.

Since buffalo *(Bubalus bubalis)* contributes immensely to the Indian agricultural economy, other animal TLR LRRs were compared with respect to buffalo. The LRR regions of TLR 1 to 10 were compared within inter species level. This comparison was feasible by using online tools like SSM, SSAP and FATCAT. In the SSM tool, the Q-score represents the quality function of Ca-alignment, maximized by the SSM alignment algorithm and the P-score represents minus logarithm of the P-value. The Z-score measures the statistical significance of a match in terms of Gaussian statistics; the root mean square deviation (RMSD) was calculated between Ca-atoms of matched residues at best 3D superposition of the query and target structures. In the FATCAT tool, the P value signifies the probability of structural similarity between the two protein structures and the no of twists denotes the transformations of the 3D proteins to obtain better alignment. In the SSAP server the overlap of structurally similar regions are denoted as the percentage of overlap.

Root-mean square deviation (RMSD) of the Cα atoms of the model structures compared to the native structure, in a globally optimized superposition of the two structures, as one of the measures of similarity to assess the models. Improper modeling of a small region of the protein can sometimes lead to large variation in RMSD [33]. Based on this aspect, the LRR regions from TLRs like 1, 2, 3 and 6 were found to be highly similar in inter species level since their RMSD deviation is less than 2 A with high relevance in statistical values. Further, the structural superimposition of these TLR's showed only marginal variations among each other. On the other hand, the TLRs like 5, 7, 8, and 9 were found to be highly dis-similar with respect to each other having higher RMSD deviation and inconsistent statistical scores. The structural overlay of TLR 5, 7, 8 and 9 showed prominent variations in their horse shape shoe structure. In few TLRs like TLR 4 structural dissimilarity exists only with respect to buffalo and goat; while in TLR 10 structural dissimilarity exhibits only with buffalo and sheep.

From the results (Table 2) and the structural view (Fig. 2, 3, 4) given as Supplementary material, it can be concluded that similar TLR LRR structures had a RMSD value of less than 2 angstrom and the dissimilar LRRs had greater RMSD deviation. A characteristic feature of TLR-ECDs in TLR 7, 8 and 9 is that frequent occurrence of LRRs forms substantially larger regions which are often represented as loops that protrude from the TLR-ECD horseshoe structure, usually on the ascending or convex side of the LRR [6]. This extra loop projection can also be seen in the TLR 7, 8 and 9 modeled structures of sheep, buffalo and bovine. The structural superimposition of TLR 2, 3 and 7 demonstrates that TLR 2, 3 have species conservation since the 3D overlay differs only by a minimal variation. But TLR 7 shows prominent differences in the structural level across the four animal species. It has been widely reported that TLR agonists are lipopolysaccharide (LPS) from gram negative bacteria (TLR4), lipoprotein and peptidoglycan from gram positive bacteria (TLR1, 2 and 6), flagellin (TLR5), double stranded RNA, Poly I:C (TLR3), unmethylated CpG dinucleotide motifs (TLR9), single stranded uridine rich RNA (TLR7) and the synthetic antiviral compound R-848 (TLR7 and TLR8).

A previous study conducted by our group indicated that upon stimulation with peptidoglycan, Toda buffaloes produced significantly increased levels of IFN γ and TNF α mRNAs. TLR 3 ligand poly I:C showed significantly increased expression in the IL 1 β, IFN γ and TNF l α mRNA levels in Toda buffaloes and imiquimod resulted in a significant increase of TNF α mRNAs levels [40]. Due to this established cytokine increased expression levels in TLR 2, 3 and 7 molecular docking studies was carried out with these TLRs against known ligand compounds like Peptidoglycan ((C32H48N6O18R2)n), Poly I:C ($C_{19}H_{27}N_7O_{16}P_2$), Resiquimod ($C_{17}H_{22}N_4O_2$) and Imiquimod ($C_{14}H_{16}N_4$). The peptidoglycan ligand from KEGG ligand database was also verified as a glycosaminoglycan structure through Chemical entity database (ChEBI: 8005). Also, the poly I:C compound (CID: 32744) was found to be the interferon inducer consisting of a synthetic, mismatched double-stranded RNA with one strand each of polyinosinic acid and polycytidylic acid (MeSH db, http://www.ncbi.nlm.nih.gov/mesh/68011070). The increased expression of IL-36γ cytokines in skin was induced upon activation with polyinosinic - polycytidylic acid (Poly I:C) which is the analogue structure for dsRNA [41]. Therefore this compound was chosen to perform the binding analysis with TLR 3. Agonists resiquimod (CHEMBL383322) and imiquimod (CHEBI:36704) was also found to be associated with increased cytokine secretion (PMID: 21780996) and can be subsequently used as vaccine adjuvants (PMID: 17931162).

All the modeled proteins of TLR 2, 3 and 7 bound with their respective ligand structures. However the binding site, the number of hydrogen bonds and electrostatic bonds varied consistently. In the human TLR3/dsRNA complex the protein-protein interactions occur only at the LRR-CT. This concept was verified in animal TLR 3 poly IC binding. While sheep and bovine TLR 3 do show interactions in the LRR-CT end, the goat and buffalo TLR 3 showed Poly IC binding in the middle of the horse shoe structure, i.e., in between LRR-NT and LRR-CT. Electrostatic and hydrophobic interactions were observed around the ligand binding site.

In Fig. 2, the bond distance and the interacting amino acids are labeled, the carbon atoms are represented as green, nitrogen as blue and oxygen as red colored type. On analyzing the docking results of TLR 2, 3, and 7 the number of hydrogen bonds varies between the TLR ligand complexes. Hydrogen bonding and optimized hydrophobic interactions help to stabilize the ligands at the target site, and enable for better binding affinity and drug efficacy [42]. Based on this phenomenon, TLR 3-poly I:C complex had better binding affinity with highest number of bond interactions than other TLRs. Further, the bond energy was found to be in the range of −2.5 to −0.01 kcal mol^{-1} and the bond distance were in the range of 2.7 to 3.57 A.

Amino acid sequences of the TLR 7–9 family suggest that they may differ from other TLRs in both structure and mode of ligand recognition [6]. This statement holds true because most of the associations of TLR 7 LRR protein (goat, buffalo and bovine) against Resiquimod and Imiquimod are shown toward the N terminal end. Sheep TLR 7 being the exceptional case. Buffalo TLR 7 docked against Resiquimod showed the most stable structure with minimal energy (Fig. 2). A study reveals that PGN can bind to the C-terminus, 572–586 end of TLR-2 [43]. In this study, peptidoglycan was found to bind between the C-terminal and N-terminal region of rumen TLR 2. While animal TLR 2 and 3 shows binding associations toward the LRR-CT end, TLR 7 alone showed binding regions around N terminal region.

Binding energy between TLR 2 of goat, buffalo, bovine with Peptidoglycan showed energy variations between −8.4 to −9.8(kcal mol^{-1}). This being the highest, other associations of TLR 3 and 7 showed ligand binding energy ranging from −6.8 to −8.1 (kcal mol^{-1}). The TLR LRRs with minimal binding energy are shown in Fig.1. The number of hydrogen bonds were lowest in the TLR 2 Peptidoglycan complex and highest in the TLR 3 Poly I:C complex. Asparagines in the motif make continuous hydrogen bonds with neighboring strands and constitute an “Asparagine ladder”. Often Asparagines are replaced with other residues to form H2 bonds [44]. This study also shows that TLR 2, 3 and TLR 7 showed active participation with Asparagine (Asn) toward hydrogen bond formations. While this docking study has been done insilico, performing thermodynamics on inclusion of water molecules are also found to be essential for ligand-receptor interactions. Future studies involving molecular dynamic simulations are needed to access the stability of the complex.

Conclusions

Detailed understanding of the structural basis for PAMP recognition and signaling by TLRs could lead to the development of adjuvants that specifically bind to TLR-ECDs and activate TLRs for anti-inflammatory drugs that block TLR mediated signaling [6]. Since there are no structural models available for TLR LRR in animal species like goat, sheep, buffalo and bovine, this study will be useful to understand the underlying PAMP recognition mechanism in animal TLRs. Species level conservation of TLR 1–10 ectodomains illustrates the similarities and dissimilarities of these protein structures across the four animal species. This analysis showed that TLR 1, 2, 3 and 6 had structural convergence while TLR 5, 7, 8 and 9 had structural divergence among the selected rumen species. Computational docking studies on TLR 2, 3 and 7 highlights the mode of ligand recognition and their bonding interactions. In summary, this work gives an insight about the structural information of animal TLRs, their species conservation and ligand recognition.

Acknowledgments The authors thank Indian Council of Agricultural Research – National Agricultural Innovation Project (NAIP) for funding this study under Project code C-2153 and Tamil Nadu Veterinary and Animal Sciences University, Chennai for extending all facilities to carry out the work.

References

1. Kumar H, Kawai T, Akira S (2009) Toll-like receptors and innate immunity. Biochem Biophys Res Commun 388:621–625
2. Yang IV, Jiang W, Rutledge HR, Lackford B, Warg LA, De Arras L, Alper S, Schwartz DA, Pisetsky DS (2011) Identification of novel innate immune genes by transcriptional profiling of macrophages stimulated with TLR ligands. Mol Immunol 48:1886–1895
3. Kubarenko AV, Ranjan S, Colak E, George J, Frank M, Weber AN (2010) Comprehensive modeling and functional analysis of Toll-like receptor ligand-recognition domains. Protein Sci 19:558–569
4. Raja A, Vignesh AR, Mary BA, Tirumurugaan KG, Raj GD, Kataria R, Mishra BP, Kumanan K (2011) Sequence analysis of Toll-like receptor genes 1–10 of goat (Capra hircus). Vet Immunol Immunopathol 140:252–258
5. Kumar H, Kawai T, Akira S (2011) Pathogen recognition by the innate immune system. Int Rev Immunol 30:16–34
6. Botos I, Segal DM, Davies DR (2011) The structural biology of Toll-like receptors. Structure 19:447–459
7. Marie EY, Lavine MD, Buetler B (2011) Toll like receptors. Curr Biol 21:R488–R493
8. Cavasotto CN, Phatak SS (2009) Homology modeling in drug discovery: current trends and applications. Drug Discov Today 14:676–683
9. Dalton JA, Jackson RM (2010) Homology-modeling protein-ligand interactions: allowing for ligand-induced conformational change. J Mol Biol 399:645–661
10. Wei T, Gong J, Jamitzky F, Heckl WM, Stark RW, Rössle SC (2009) Homology modeling of human Toll-like receptors TLR7, 8, and 9 ligand-binding domains. Protein Sci 18:1684–1691
11. Govindaraj RG, Manavalan B, Lee G, Choi S (2010) Molecular modeling-based evaluation of hTLR10 and identification of potential ligands in Toll-like receptor signaling. PLoS One 5(9):e12713
12. Wei T, Gong J, Rössle SC, Jamitzky F, Heckl WM, Stark RW (2011) A leucine-rich repeat assembly approach for homology modeling of the human TLR5-10 and mouse TLR11-13 ectodomains. J Mol Model 17:27–36

13. Sali A, Potterton L, Yuan F, van Vlijmen H, Karplus M (1995) Evaluation of comparative protein modeling by MODELLER. Proteins 23(3):318–326
14. Larkin MA, Blackshields G, Brown NP, Chenna R, McGettigan PA, McWilliam H, Valentin F, Wallace IM, Wilm A, Lopez R, Thompson JD, Gibson TJ, Higgins DG (2007) Clustal W and Clustal X version 2.0. Bioinformatics 23:2947-8Laskowski RA, Moss DS, Thornton JM (1993) Main-chain bond lengths and bond angles in protein structures. J Mol Biol 231:1049-67.
15. Laskowski RA, Moss DS, Thornton JM (1993) Main-chain bond lengths and bond angles in protein structures. J Mol Biol 231: 1049–1067
16. Colovos C, Yeates TO (1993) Verification of protein structures: patterns of nonbonded atomic interactions. Protein Sci 2:1511–1519
17. Bowie JU, Luthy R, Eisenberg D (1991) A method to identify protein sequences that fold into a known three-dimensional structure. Science 253:164–170
18. Hekkelman ML, Te Beek TA, Pettifer SR, Thorne D, Attwood TK, Vriend G (2010) WIWS: a protein structure bioinformatics Web service collection. Nucleic Acids Res 38:W719–W723
19. Wallner B, Elofsson A (2003) Can correct protein models be identified? Protein Sci 12:1073–1086
20. Castrignanò T, De Meo PD, Cozzetto D, Talamo IG, Tramontano A (2006) The PMDB Protein Model Database. Nucleic Acids Res 34:D306–D309
21. Kelley LA, Shrimpton PJ, Muggleton SH, Sternberg MJ (2009) Discovering rules for protein-ligand specificity using support vector inductive logic programming. Protein Eng Des Sel 22:561–567
22. Chang DT, Chen CY, Chung WC, Oyang YJ, Juan HF, Huang HC (2004) ProteMiner-SSM: a web server for efficient analysis of similar protein tertiary substructures. Nucleic Acids Res 32:W76–W82
23. Harrison A, Pearl F, Sillitoe I, Slidel T, Mott R, Thornton J, Orengo C (2003) Recognizing the fold of a protein structure. Bioinformatics 19:1748–1759
24. Ye Y, Godzik A (2004) FATCAT: a web server for flexible structure comparison and structure similarity searching. Nucleic Acids Res 32:W582–W585
25. Seabury CM, Cargill EJ, Womack JE (2007) Sequence variability and protein domain architectures for bovine Toll-like receptors 1, 5, and 10. Genomics 90:502–515
26. Kim HM, Oh SC, Lim KJ, Kasamatsu J, Heo JY, Park BS, Lee H, Yoo OJ, Kasahara M, Lee JO (2007) Structural diversity of the hagfish variable lymphocyte receptors. J Biol Chem 282:6726–6732
27. Pancer Z, Cooper MD (2006) The evolution of adaptive immunity. Annu Rev Immunol 24:497–518
28. Meng G, Grabiec A, Vallon M, Ebe B, Hampel S, Bessler W, Wagner H, Kirschning CJ (2003) Cellular recognition of tri-/di-palmitoylated peptides is independent from a domain encompassing the N-terminal seven leucine-rich repeat (LRR)/ LRR-like motifs of TLR2. J Biol Chem 278:39822–39829
29. Brodsky I, Medzhitov R (2007) Two modes of ligand recognition by TLRs. Cell 130:979–981
30. Jin MS, Lee JO (2008) Structures of the toll-like receptor family and its ligand complexes. Immunity 29:182–191
31. Watanabe T, Tokisue T, Tsujita T, Matsumoto M, Seya T, Nishikawa S, Hasegawa T, Fukuda K (2007) N-terminal binding site in the human toll-like receptor 3 ectodomain. Nucleic Acids Symp Ser (Oxf) 51:405–406
32. Bell JK, Botos I, Hall PR, Askins J, Shiloach J, Segal DM, Davies DR (2005) The molecular structure of the Toll-like receptor 3 ligand-binding domain. Proc Natl Acad Sci USA 102:10976–10980
33. Iavarone C, Ramsauer K, Kubarenko AV, Debasitis JC, Leykin I, Weber AN, Siggs OM, Beutler B, Zhang P, Otten G, D'Oro U, Valiante NM, Mbow ML, Visintin A (2011) A point mutation in the amino terminus of TLR7 abolishes signaling without affecting ligand binding. J Immunol 186:4213–4222
34. Reddy CS, Vijayasarathy K, Srinivas E, Sastry GM, Sastry GN (2006) Homology modeling of membrane proteins: a critical assessment. Comput Biol Chem 30:120–126
35. Dalton JA, Jackson RM (2007) An evaluation of automated homology modeling methods at low target template sequence similarity. Bioinformatics 23:1901–1908
36. Reddy BV, Kaznessis YN (2007) Use of secondary structural information and C alpha-C alpha distance restraints to model protein structures with MODELLER. J Biosci 32:929–936
37. Hooft RW, Sander C, Vriend G (1997) Objectively judging the quality of a protein structure from a Ramachandran plot. Comput Appl Biosci 13:425–430
38. Benkert P, Biasini M, Schwede T (2011) Toward the estimation of the absolute quality of individual protein structure models. Bioinformatics 27:343–350
39. Eisenberg D, Lüthy R, Bowie JU (1997) VERIFY3D: assessment of protein models with three-dimensional profiles. Methods Enzymol 277:396–404
40. Vignesh AR, Dhinakar Raj G, Dhanasekaran S, Tirumurugaan KG, Raja A (2012) Comparative in vitro toll-like receptor ligand induced cytokine profiles of Toda and Murrah buffaloes-Identification of tumour necrosis factor alpha promoter polymorphism. Vet Immunol Immunopathol 150:189–197
41. Lian LH, Milora KA, Manupipatpong KK, Jensen LE (2012) The double-stranded RNA analogue polyinosinic-polycytidylic acid induces keratinocyte pyroptosis and release of IL-36γ. J Invest Dermato 132:1346–1353
42. Patil R, Das S, Stanley A, Yadav L, Sudhakar A, Varma AK (2010) Optimized hydrophobic interactions and hydrogen bonding at the target-ligand interface leads the pathways of drug-designing. PLoS One 5(8):e12029
43. Li Y, Efferson CL, Ramesh R, Peoples GE, Hwu P, Ioannides CG (2011) A peptidoglycan monomer with the glutamine to serine change and basic peptides bind in silico to TLR-2 (403–455). Cancer Immunol Immunother 60:515–524
44. Werling D, Jann OC, Offord V, Glass EJ, Coffey TJ (2009) Variation matters: TLR structure and species-specific pathogen recognition. Trends Immunol 30:124–130